Klein-Gordon equation on a Lagrange mesh

Daniel Baye*

Nuclear Physics and Quantum Physics, C.P. 229, Université Libre de Bruxelles (ULB), B-1050 Brussels Belgium

(Received 5 February 2024; accepted 25 March 2024; published 10 April 2024)

The Lagrange-mesh method is an approximate variational method which provides accurate solutions of the Schrödinger equation for bound-state and scattering few-body problems. The stationary Klein-Gordon equation depends quadratically on the energy. For a central potential, it is solved on a Lagrange-Laguerre mesh by iteration. Results are tested with the Coulomb potential for which exact solutions are available. A high accuracy is obtained with a rather small number of mesh points. For various potentials and levels, few iterations provide accurate energies and mean values in short computer times. Analytical expressions of the wave functions are available.

DOI: 10.1103/PhysRevE.109.045303

I. INTRODUCTION

The Lagrange-mesh method [1–3] is very successful to accurately solve the Schrödinger equation in a number of problems in quantum mechanics. It gives highly accurate results with rather few mesh points for bound and scattering properties of various two- and three-body systems (see Ref. [3] and references therein). As it is economical in the number of mesh points, it is particularly useful to reduce computer times when the computation of matrix elements is very heavy, such as in descriptions of nuclear collisions and reactions [4–8]. High accuracies can be obtained for three-body atoms, molecules, and exotic systems [9–12]. The method is also efficient to solve the Dirac equation and use its wave functions [13–16]. The numerical treatment of the mesh equations in all these problems relies on standard linear algebra.

The Lagrange-mesh method is an approximate variational calculation involving a set of N functions associated with N mesh points [1,3]. All matrix elements are calculated with the Gauss quadrature associated with this mesh. The Lagrange variational basis involves infinitely differentiable functions vanishing at all points of the mesh, except one. The simplicity of the method arises from the fact that the potential is represented by the diagonal matrix of its values at mesh points. The kinetic energy matrix is nondiagonal but sparse when several variables occur. In spite of this simplicity, high accuracies can be achieved with small numbers of mesh points [3,17]. Remarkably, this method can give numerically exact energies and mean values for a Coulomb potential in both the Schrödinger and Dirac cases [3,13].

The aim of the present paper is to show that the Lagrange-mesh method can also be used to solve the stationary Klein-Gordon equation [18,19], where the energy appears in quadratic form. The Klein-Gordon equation describes the relativistic behavior of spin-zero particles such as pions. With a central potential, it is solved on a Lagrange mesh based on zeros of Laguerre polynomials. The quadratic dependence on the energy is treated with a simple iteration. The corresponding Schrödinger equation is first solved on the same mesh to provide information about optimal conditions for the calculation. Then, using the nonrelativistic eigenvalue as a starting point, the Klein-Gordon equation is solved by iteration.

The Lagrange-mesh method is summarized in Sec. II. The case of the Klein-Gordon equation is treated in Sec. III. Numerical applications for the Coulomb potential and various singular and nonsingular potentials are described in Sec. IV. Concluding remarks are presented in Sec. V. An Appendix summarizes exact analytical expressions in the Coulomb case.

II. LAGRANGE-MESH METHOD

The Lagrange-mesh method introduced in Ref. [1] has been developed and extended over the years [2,17,20]. A general presentation is given in Ref. [3].

In this section, the method is summarized in the one-dimensional case. Let us consider Hamiltonian

$$H = -\frac{\hbar^2}{2m}\frac{d^2}{dx^2} + V(x) \tag{1}$$

for a particle of mass m in a potential $V(x)$ defined over interval $[a, b]$. An approximate variational calculation is performed with a basis of N infinitely differentiable Lagrange functions $f_j(x)$ associated with a set of N mesh points x_i. These mesh points correspond to a quadrature rule

$$\int_a^b g(x)\,dx \approx \sum_{k=1}^{N} \lambda_k g(x_k), \tag{2}$$

with weights λ_k. Expression (2) is hereafter named Gauss quadrature even when it is a generalization of the standard definition [21,22]. Functions f_j verify the Lagrange property

$$f_j(x_i) = \lambda_i^{-1/2}\delta_{ij}, \tag{3}$$

which is inspired by Lagrange interpolation, i.e., they vanish at all mesh points but one. With the Gauss quadrature (2) and property (3), the functions f_j form an approximately

*daniel.baye@ulb.be

orthonormal set over $[a, b]$:

$$\langle f_i|f_j\rangle = \int_a^b f_i(x)f_j(x)dx \approx \sum_{k=1}^{N} \lambda_k f_i(x_k)f_j(x_k) = \delta_{ij}. \quad (4)$$

In particular cases, the orthonormality of the Lagrange functions can be exact.

With this Lagrange basis, an approximate variational calculation is performed for H where all matrix elements are computed with the Gauss quadrature (2) as indicated by a label G. The wave function is expanded as

$$\psi(x) = \sum_{j=1}^{N} c_j f_j(x). \quad (5)$$

The obtained equations take the meshlike form

$$\sum_{j=1}^{N} \left(\frac{\hbar^2}{2m} T_{ij}^G + V(x_i)\delta_{ij} \right) c_j = E c_i. \quad (6)$$

The kinetic energy matrix involves the simple expression

$$T_{ij}^G = \langle f_i| - d^2/dx^2|f_j\rangle_G = -\lambda_i^{1/2} f_j''(x_i). \quad (7)$$

When this approximation is not symmetrical like the exact T_{ij}, one can also use the slightly more complicated

$$T_{ij}^G = \sum_{k=1}^{N} \lambda_k f_i'(x_k) f_j'(x_k). \quad (8)$$

The crucial advantage of the method is that the potential energy matrix is diagonal with the Lagrange property (3),

$$\langle f_i|V(x)|f_j\rangle_G = V(x_i)\delta_{ij}, \quad (9)$$

and very simple. The calculation is thus reduced to a standard problem of linear algebra.

In spite of its simplicity, the Lagrange-mesh method can be extremely accurate. The most striking property is that the accuracy on a number among the lowest energies can be orders of magnitude better than the accuracy of individual matrix elements [17]. In fact, various examples of comparison with the standard variational method using the same Lagrange basis, i.e., with exact calculations of all matrix elements, have shown that the Gauss quadrature approximation does not cost any significant loss of accuracy for the lowest eigenvalues [3,17]. Nevertheless, the validity of the method depends on the accuracy of the Gauss rule. This means that discontinuities or singularities in the potential or some of its first derivatives may destroy the interest of the method.

The above simple presentation emphasizes the spirit of the Lagrange-mesh method. The method is, in fact, much more general. It has been extended to many types of applications: studies of continuum and collisions, coupled channels reactions, three-body atoms and molecules, confined systems, Dirac equation, etc. To this end, various generalizations involving changes of variables and extensions of basis functions had to be introduced. The most important one is the regularization technique explained below in a particular case.

Most applications of the Lagrange-mesh method involve Lagrange functions based on classical orthogonal polynomials [21]. Other types, however, exist based on nonclassical polynomials or on periodic functions. The choice of Lagrange mesh depends on the interval on which the potential is defined and on the behavior of this potential at the extremities of this interval. In some cases, the Lagrange-mesh equations present similarities with or are even equivalent to those in other meshlike methods such as the discrete-variable representation [23] also based on classical polynomials or the quadrature discretization method [24] based on nonclassical polynomials (see Ref. [3] for details).

The Lagrange-mesh method is of particular interest for infinite or semi-infinite intervals since convenient Lagrange bases are available on such intervals. Let me now take the example of interval $[0, \infty]$, which is of interest for the next sections. The corresponding classical orthogonal polynomials are the Laguerre polynomials $L_N^\alpha(x)$. The N mesh points x_i are defined by

$$L_N^\alpha(x_i) = 0. \quad (10)$$

They depend on the choice for α. The Lagrange-Laguerre functions are

$$f_j(x) = (-1)^j x_j^{1/2} \left(h_N^\alpha\right)^{-1/2} \frac{L_N^\alpha(x)}{x - x_j} x^{\alpha/2} e^{-x/2}. \quad (11)$$

They vanish at all $x_i \neq x_j$. Factor $x^{\alpha/2}e^{-x/2}$ is the square root of the weight function related to the Laguerre polynomials and $h_N^\alpha = \Gamma(N + \alpha + 1)/N!$ is the squared norm of L_N^α [21]. These functions are exactly orthonormal over $[0, \infty]$. The Gauss quadrature in Eq. (4) is exact in this case, as the integrand is the product of the weight function by a polynomial of degree strictly smaller than $2N$ [22]. Parameter α is selected so the factor $x^{\alpha/2}$ fits the expected behavior of the wave function near the origin.

These Lagrange functions have the drawback that the Gauss-Laguerre quadrature is inaccurate for matrix elements of operators presenting a singularity at the origin such as the centrifugal term $\hbar^2 l(l+1)/2mr^2$ or the Coulomb potential $-e^2/r$ [1]. This problem can be solved with a regularization [2,3,17].

Regularized Lagrange functions are defined as

$$\hat{f}_j(x) = \frac{x}{x_j} f_j(x). \quad (12)$$

These functions still satisfy the Lagrange conditions (3). They are *not* orthogonal but are still orthonormal at the Gauss-Laguerre quadrature approximation. Strikingly, treating them as if they were orthonormal does not induce additional inaccuracy [3,17]. With the regularization, matrix elements of operators presenting a singularity at most x^{-2} at the origin are now accurate with the Gauss quadrature. Matrix elements of the kinetic energy operator $-d^2/dx^2$ are obtained from Eq. (7) by a double differentiation of $\hat{f}_j(x)$ as [3,20]

$$\hat{T}_{ij}^G = (-1)^{i-j} \frac{x_i + x_j}{\sqrt{x_i x_j}(x_i - x_j)^2} \quad (13)$$

for $i \neq j$ and

$$\hat{T}_{ii}^G = -\frac{1}{12x_i^2}\left[x_i^2 - 2(2N + \alpha + 1)x_i + \alpha^2 - 4\right] \quad (14)$$

for $i = j$. With these simple expressions, approximate energies and wave functions of the Schrödinger equation are

obtained by solving system (6). In practice, it is important to introduce a scale factor in the Lagrange functions to optimize the mesh as explained in the next section.

III. EXTENSION TO THE KLEIN-GORDON EQUATION

The time-independent Klein-Gordon equation for a particle with energy E in a potential V is given in relativistic units $\hbar = c = m = 1$, where m is the particle mass, by [19]

$$[-\Delta - (E - V)^2 + 1]\psi(\boldsymbol{r}) = 0. \tag{15}$$

For a central potential $V(r)$, with $\psi_{lm}(\boldsymbol{r}) = Y_{lm}(\theta, \varphi)r^{-1}u_l(r)$, the radial Klein-Gordon equation for a given value of the orbital momentum l reads

$$\left\{-\frac{d^2}{dr^2} + \frac{l(l+1)}{r^2} - [E - V(r)]^2 + 1\right\}u_l(r) = 0. \tag{16}$$

The energy appears in quadratic form and requires an extension of the treatment of Schrödinger equations.

At the origin, the solutions behave as

$$u_l(r) \underset{r \to 0}{\sim} r^{\gamma}. \tag{17}$$

For central potentials regular at the origin, $V(r) \underset{r\to 0}{\to} v_0 + O(r)$, one has $\gamma = l + 1$. For potentials with a singularity of type $V(r) \underset{r\to 0}{\to} v_{-1}r^{-1} + v_0 + O(r)$, γ is given by the real expression

$$\gamma = \tfrac{1}{2} + \sqrt{\left(l + \tfrac{1}{2}\right)^2 - (v_{-1})^2} \tag{18}$$

provided that $|v_{-1}| < l + 1/2$. In particular, for the attractive Coulomb potential

$$V(r) = -\frac{Z\alpha}{r}, \tag{19}$$

where α is the fine structure constant, it is given by

$$\gamma = \tfrac{1}{2} + \sqrt{\left(l + \tfrac{1}{2}\right)^2 - (Z\alpha)^2} \tag{20}$$

with the condition $Z\alpha < l + 1/2$. At large r, the bound-state radial functions decrease exponentially when the potential vanishes at infinity and decrease faster than exponentially for confining potentials.

To numerically determine bound-state energies, an iterative method is used on a Lagrange mesh. First, Eq. (16) is rewritten as

$$\left\{-\frac{1}{2}\frac{d^2}{dr^2} + \frac{l(l+1)}{2r^2} + V(r) - \frac{1}{2}[E - 1 - V(r)]^2\right\}u_l(r) = (E - 1)u_l(r). \tag{21}$$

The eigenvalue is the energy $E - 1$ without mass energy. Without the quadratic term, Eq. (21) reduces to the Schrödinger equation.

The radial wave function of bound states is expanded over the regularized basis (12) as

$$u_l(r) = h^{-1/2}\sum_{j=1}^{N} c_{lj}\hat{f}_j(r/h), \tag{22}$$

where a scale parameter h is introduced to allow an optimization of the mesh. Radial function u_l is normed at the Gauss-Laguerre approximation if $\sum_j c_{lj}^2 = 1$. The N zeros x_j of polynomial $L_N^{\alpha'}(x)$ define the Lagrange mesh points hx_j, depending on h and α'. To ensure a fast convergence, α' must be chosen so as to mimic the appropriate behavior (17) at the origin. This is achieved with

$$\alpha' = 2(\gamma - 1). \tag{23}$$

A similar choice was proven convenient in the Lagrange-mesh treatment of the Dirac equation, especially in the case of a singular potential [13]. Parameter h will be selected by searching a plateau of stationary energies. For a first guess, this search can be performed on the Schrödinger equation. Choosing a nearly optimal h can lead to a significant reduction of the number N of mesh points.

Using the Lagrange-Laguerre basis as a variational basis together with the associated Gauss approximation, one obtains the system

$$\sum_{j=1}^{N}\left\{\frac{1}{2h^2}\hat{T}_{ij}^{G} + \left[\frac{l(l+1)}{2(hx_i)^2} + V(hx_i) - \frac{1}{2}[E - 1 - V(hx_i)]^2\right]\delta_{ij}\right\}c_{lj} = (E - 1)c_{li}. \tag{24}$$

The simplicity of Eq. (24) comes from the fact that the approximations of the centrifugal term and powers of the potential are diagonal and simple. In fact, the matrix elements of the centrifugal term and of a Coulomb potential and its square are exact.

If the potential is small with respect to the mass energy, the quadratic term in Eq. (24) is small with respect to unity. Let $E_0 - 1$ be the nonrelativistic eigenvalue obtained with the Schrödinger equation corresponding to this potential, i.e., with Eq. (24) without quadratic term. The small nonlinear term $\frac{1}{2}[E - 1 - V(hx_i)]^2$ is replaced by $\frac{1}{2}[E_0 - 1 - V(hx_i)]^2$. The resulting linear system then provides an energy E_1. Proceeding similarly with E_1 replacing E gives E_2 and so on. After i iterations, an accurate converged eigenvalue $E = E_i$ is obtained when $|(E_i - E_{i-1})/(E_i - 1)|$ is smaller than a given $\epsilon > 0$. After roughly optimizing the scale parameter h, the calculation can be performed with rather small numbers N of mesh points and is thus fast.

The method is valid when the potential is not too strong with respect to the mass energy mc^2. It was verified numerically that iterations do not converge for some strong potentials. Nevertheless, examples below show that the method is valid even in cases where relativistic corrections can be important.

When a chosen accuracy of the energy is reached, radial wave functions are obtained in analytical form with Eq. (22). The quality of this wave function can be tested on mean values. The average of operators $O(r)$ depending on the radial coordinate are obtained with the Gauss quadrature as

$$\langle O(r)\rangle = \sum_{j=1}^{N} c_{lj}^2 O(hx_j), \tag{25}$$

where the c_{lj} are the coefficients in expansion (22). As shown below, their accuracy is not far from the accuracy of the energy.

TABLE I. Binding energies $E_{n_r l} - 1$ in scaled atomic units $(n/Z)^2 E_\mathrm{h}$ for the Coulomb potential obtained with N mesh points and $h = n/2Z$ after i iterations compared with exact values for $Z = 1$, 50, and 100.

				$E_{n_r l} - 1$ in units $(n/Z)^2 E_\mathrm{h}$		
Z	n_r	l	i	$N = 10$	$N = 20$	Exact
1	0	0	4	−0.500033285818945	−0.500033285818945	−0.500033285818947
	1	0	3	−0.500021635367954	−0.500021635367952	−0.500021635367954
	0	1	3	−0.500003882960090	−0.500003882960091	−0.500003882960089
	9	0	3	−0.5000102	−0.500005125764849	−0.500005125764849
	0	9	3	−0.500000080577731	−0.500000080577731	−0.500000080577731
50	0	0	14	−0.619462444705755	−0.619462444705763	−0.619462444705754
	1	0	9	−0.572738939702176	−0.572738939702173	−0.572738939702176
	0	1	9	−0.510024493439603	−0.510024493439598	−0.510024493439604
	9	0	5	−0.528	−0.515665188121745	−0.515665188121744
	0	9	5	−0.500201593871028	−0.500201593871027	−0.500201593871029
100	0	1	13	−0.544604007143506	−0.544604007143500	−0.544604007143506
	8	1	6	−0.51742	−0.517353686579109	−0.517353686579107
	0	9	6	−0.500808177370508	−0.500808177370508	−0.500808177370508

IV. APPLICATIONS

A. Coulomb potential

A first application is for the Coulomb potential (19). As exact results are available, it provides accurate tests of the method.

The Lagrange-Laguerre functions (12) are optimal in this case as analytical wave functions can be exactly represented with expansion (22) as well in the Schrödinger case [2,3] as in the Dirac [3,13] and Klein-Gordon cases [see Eq. (A3)]. Parameter α' in the Laguerre polynomial is given by Eqs. (23) and (20). This value is not optimal for the calculation of the initial value E_0 as the nonrelativistic wave functions behave as r^{l+1} near the origin. Nevertheless, this nonoptimal E_0 does not cost additional iterations in practice. A fair value for the scale parameter h is suggested by the exponential term $\exp(-Zr/n)$ of the nonrelativistic exact solution, i.e., $h = n/2Z$, where $n = n_r + l + 1$ is the principal quantum number.

Typical binding energies $E_{n_r l} - 1$ of various levels with radial quantum number n_r and orbital momentum l are displayed in Table I for $N = 10$ and 20 and compared with their exact value (A6). In units of scaled Hartrees $(n/Z)^2 E_\mathrm{h}$, they can also be easily compared with their common nonrelativistic value -0.5. For the fine structure constant, the CODATA 2020 value $1/\alpha = 137.035999084$ is used [25]. One observes that excellent results with an accuracy better than 10^{-14} are obtained with $N = 10$ as well for the $1s$, $2s$, and $2p$ levels, as for the $l = 9$ level of the $n = 10$ shell, i.e., when the number n_r of nodes in the wave function is small. Not surprisingly, $N = 10$ is too small when the radial function has nine nodes as in the $10s$ state but the result with $N = 20$ is accurate. In the absence of known exact results, the accuracy can be established by a comparison of successive N values.

These comments are valid for both $Z = 1$ and $Z = 50$. The main difference lies in the number of iterations which is larger for $Z = 50$. For $Z = 50$, one observes a decrease of this number with n, consistent with the decrease of relativistic effects with increasing n. Interestingly, the same comments apply for $Z = 100$ with $l > 0$ given that Eq. (16) with $l = 0$ is not valid for $Z > 68$.

The accuracy of the wave functions is analyzed for the ground state in Table II on scaled mean values $\langle r^k \rangle$ of various powers k of the radial coordinate in scaled Bohr radii a_0/Z. The nonrelativistic values corresponding to $k = -2$, -1, 1, and 2 are 2, 1, 3/2, and 3, respectively. The comparison between results obtained with $N = 10$ and 20 as well as the comparison with exact results indicate an accuracy better than 10^{-13} for both Z values. Relativistic corrections

TABLE II. Mean values in scaled Bohr radii a_0/Z of the $1s$ ground state obtained with N mesh points and i iterations compared with exact values [Eqs. (A7)–(A10)] for $Z = 1$ and 50.

Z	i	$\langle r^k \rangle$	$N = 10$	$N = 20$	Exact
1	4	$\langle r^{-2} \rangle$	2.00042609592427	2.00042609592424	2.00042609592428
		$\langle r^{-1} \rangle$	1.00007988660364	1.00007988660363	1.00007988660364
		$\langle r \rangle$	1.49990680605283	1.49990680605282	1.49990680605283
		$\langle r^2 \rangle$	2.99965386052346	2.99965386052342	2.99965386052345
50	14	$\langle r^{-2} \rangle$	4.12724897476497	4.12724897476482	4.12724897476496
		$\langle r^{-1} \rangle$	1.29460235128804	1.29460235128802	1.29460235128804
		$\langle r \rangle$	1.23120394276805	1.23120394276804	1.23120394276805
		$\langle r^2 \rangle$	2.08069763475680	2.08069763475678	2.08069763475681

TABLE III. Binding energy for the Yukawa potential $-\exp(-r/4)/4r$ as a function of N and i with $h = 2.7$ in relativistic units. A nonrelativistic result is displayed as NR.

N	i	$E_{00} - 1$	$\langle 1/r \rangle$	$\langle r \rangle$
10	8	−0.001292029	0.14712	12.995
20	8	−0.0012920485675	0.1470917926	13.0082342
30	8	−0.001292048566705	0.14709179167273	13.00823500274
40	8	−0.001292048566704	0.14709179167267	13.008235002767
50	8	−0.001292048566705	0.14709179167270	13.008235002763
50	NR	−0.000642861874375	0.11455274906335	17.466819322455

are important for $Z = 50$. Similar comments apply for other states.

B. Yukawa potential

The next applications are singular and nonsingular cases where exact solutions are not available. The first step consists of choosing α' and the scale parameter h. A preliminary search of an optimal domain for this parameter can be performed with the Schrödinger equation. Such a domain may depend on the accuracy requested on the eigenvalues. This does not mean that h is optimal for the Klein-Gordon equation but it is often close to optimal and can be used as such or as a starting point. When E is roughly known, a first guess of h may also be given by comparing the exponential asymptotic behavior $\exp(-\sqrt{1-E^2}\,r)$ of solutions of the Klein-Gordon equation with the exponential $\exp(-r/2h)$ in the Lagrange functions. From now on, relativistic units are used throughout.

The Yukawa potential

$$V(r) = -\frac{e^{-r/4}}{4r} \tag{26}$$

is another example of singular potential. Here the coefficient of the singularity is $v_{-1} = -1/4$. For $l = 0$, parameter α' is equal to $\frac{1}{2}\sqrt{3} - 1 \approx -0.134$ according to Eqs. (23) and (18). The absolute accuracy of the lowest eigenvalue reaches 10^{-7} for h in interval [2.7,2.8] with $N = 10$, 10^{-11} for $h \in [2.5, 2.8]$ with $N = 20$, and 10^{-15} for $h \in [2.4, 2.9]$ with $N = 30$.

Binding energies $E_{00} - 1$ are presented for $h = 2.7$ in Table III for various N values. They are obtained after eight iterations. The accuracy of the wave functions is similar. The number of stable significant digits can be checked on $\langle 1/r \rangle$ and $\langle r \rangle$. For this h value, an accuracy 10^{-15} on these mean values is obtained with $N \geqslant 40$.

The corresponding nonrelativistic energy is given in Table III for $N = 50$. This binding energy is underestimated by a factor of 2 with respect to the relativistic result. The mean values indicate that the relativistic increase of binding energy corresponds to a more compact wave function. The relativistic and nonrelativistic wave functions u_{00} are shown in Fig. 1. One observes that the Klein-Gordon solution is indeed concentrated at smaller distances. Another difference not visible on the figure is that the full relativistic wave function $\psi_{00}(\boldsymbol{r})$ is singular at the origin.

No other bound state was found.

C. Gaussian potential

Let us proceed with the Gaussian potential

$$V(r) = -e^{-r^2/2}. \tag{27}$$

This potential is not singular, and standard Laguerre polynomials ($\alpha' = 0$) are used for $l = 0$.

Binding energies are presented for the optimal value $h = 0.37$ as a function of N in Table IV. They are obtained after 20 iterations. An exponential convergence is clearly observed. A relative accuracy of about 10^{-13} is obtained for $N = 50$. A similar accuracy is reached for the mean values $\langle 1/r \rangle$ and $\langle r \rangle$.

The relativistic and nonrelativistic radial functions u_{00} exhibit the same differences of shapes as in Fig. 1 with different scales. They are therefore not shown.

No other bound state was found.

D. Regularized Coulomb potential

The regularized Coulomb potential

$$V(r) = -\frac{\mathrm{erf}(r)}{r} \tag{28}$$

is nonsingular. It schematizes the potential of a pion in the Coulomb field of a very heavy nucleus. The Coulomb potential is regularized because of the finite extension of the nucleus. A realistic situation would require also taking into account the nuclear interaction between the pion and the nucleus.

The mesh is defined with $\alpha' = 2l$ since $\gamma = l + 1$. Binding energies of different levels are presented in Table V. For the

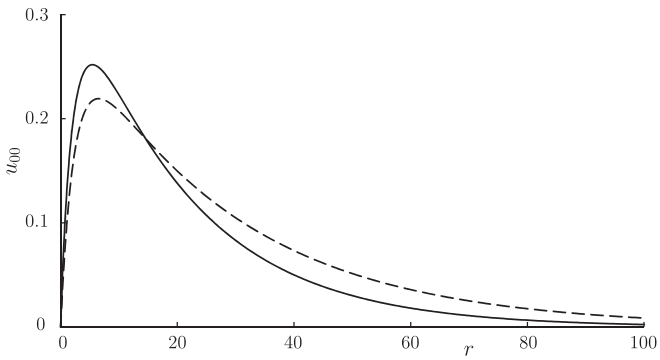

FIG. 1. Ground-state wave functions $u_{00}(r)$ of the Yukawa potential from the Klein-Gordon equation (full line) and from the Schrödinger equation (dashed line).

TABLE IV. Binding energy for the Gaussian potential $-\exp(-r^2/2)$ as a function of N and i with $h = 0.37$ in relativistic units. A nonrelativistic result is displayed as NR.

N	i	$E_{00} - 1$	$\langle 1/r \rangle$	$\langle r \rangle$
10	20	−0.088698	0.724682	2.0610
20	20	−0.088705817	0.72468942	2.0616372
30	20	−0.088705807362	0.7246893715	2.0616373554
40	20	−0.08870580735626	0.7246893713289	2.0616373555808
50	20	−0.08870580735616	0.72468937132785	2.0616373555822
50	NR	−0.03771621282652	0.57100402817655	2.7577220089962

ground state, the optimal value is $h = 0.25$. An accuracy close to 10^{-15} is already obtained for $N = 30$ after 19 iterations. Like in other cases, the relativistic binding energy is larger than in the nonrelativistic approximation and the wave functions are more compact.

With the same $h = 0.25$, fair results are obtained for the $n_r l = 10$ and 01 excited states but the accuracy is less good. The number of iterations is smaller than for the ground state. Two more correct digits arise when h is increased to about 0.32. This increase of the scale parameter is expected since the wave functions decrease more slowly in the asymptotic region and are therefore more extended than for the ground state. The convergence is a little faster for 01 than for 10 as the u_{01} radial function has no node.

The same highly excited states as for the Coulomb case in Table II are considered in Table V. The differences between low and high l are here important. While the optimal $h = 4.3$ for the 09 level is not far from the simple guess explained before the Yukawa example, the optimal $h \approx 1.2$ for the 90 level is quite different because of the many nodes of the radial function. Excellent accuracy is obtained after a few iterations but requires 100 mesh points for $l = 0$ and $n_r = 9$. On the contrary, $N = 10$ is sufficient for $l = 9$ and $n_r = 0$ since the centrifugal barrier cancels the difference with the pure Coulomb potential. For high l, nonrelativistic values are very close to exact Coulomb values.

As in other examples, the relativistic radial function is more compact than the nonrelativistic one.

V. CONCLUDING REMARKS

This paper presents an extension of the Lagrange-mesh method to a case where the eigenvalue does not appear linearly. It is hoped that it will open the way to applications of the Lagrange-mesh method beyond quantum mechanics. It could be specially useful for problems where coordinates are defined in infinite or semi-infinite intervals.

The Klein-Gordon equation is solved on a Lagrange-Laguerre mesh and the quadratic dependence on the eigenvalue is treated with an iteration. The method is efficient for potentials singular or nonsingular at the origin provided the potential is not too strong with respect to the mass energy

TABLE V. Binding energies of various levels for potential $-\mathrm{erf}(r)/r$ as a function of N, h, and i in relativistic units. Nonrelativistic results are displayed as NR.

n_r	l	N	h	i	$E_{n_r l} - 1$	$\langle 1/r \rangle$	$\langle r \rangle$
0	0	20	0.25	19	−0.372897347180	0.68477904145	2.0366141749
		30		19	−0.37289734718778	0.68477904137430	2.0366141757043
		40		19	−0.37289734718781	0.68477904137433	2.0366141757042
		40	0.25	NR	−0.33114071792649	0.61674707364291	2.2341042851891
1	0	40	0.25	13	−0.1176363446407	0.22190111329	6.42088489911956
		20	0.32	13	−0.11763621	0.221904	6.42069
		30		13	−0.117636344639	0.22190111335	6.420884900
		40		13	−0.117636344641828	0.22190111325055	6.420884903242
		40	0.32	NR	−0.101446603058818	0.19715766101250	7.371331670215
0	1	40	0.25	16	−0.138696257922225	0.28149554290709	4.471476941398
		20	0.32	16	−0.1386962567	0.28149558	4.4714746
		30		16	−0.13869625792225	0.2814955429074	4.47147694138
		40		16	−0.138696257922229	0.28149554290695	4.471476941412
		40	0.32	NR	−0.122794944077784	0.24137677361672	5.1292270331795
9	0	80	1.2	7	−0.005061801508	0.00994518576	148.27255727
		90		7	−0.0050618015100	0.0099451857558	148.272557430
		100		7	−0.00506180150967	0.0099451857551	148.2725574395
		100	1.2	NR	−0.00479018046176	0.0095292904592	156.5652731809
0	9	10	4.3	6	−0.005015216501087	0.01005571217925	104.4446452292
		20		6	−0.005015216501088	0.0100557121792749	104.44464522897
		20	4.3	NR	−0.005000000000000	0.0999999999999991	105.00000000000

of the particle. Tests performed with the Coulomb potential for which exact solutions are available confirm the validity of the method. A high accuracy is obtained with rather small numbers of mesh points. Applications to singular or nonsingular potentials and various levels are successful with small numbers of iterations. Computer times are short because of the small size of matrices required in the Lagrange-mesh method.

This mesh method also provides accurate approximations of the wave functions in analytical form. Like for the Dirac equation, such functions are easy to handle and can be used, e.g., in calculations of electromagnetic transitions [15], polarizabilities [14], and other properties. When used in Gauss quadratures, they lead to simple compact expressions.

APPENDIX : SUMMARY OF EXACT PROPERTIES FOR THE COULOMB CASE

In this Appendix, the analytical energies $E_{n_r l}$ and radial wave functions $u_{n_r l}$ of the Klein-Gordon equation with the Coulomb potential (19) are presented in relativistic units, i.e., $\hbar/mc$ for the radial coordinate and mc^2 for the energy. Convenient notations allowing an easy comparison with nonrelativistic expressions are

$$\nu = n_r + \gamma \tag{A1}$$

and

$$\mathcal{N} = \sqrt{\nu^2 + Z^2\alpha^2}, \tag{A2}$$

where γ is given by Eq. (20). Both ν and $\mathcal{N}$ become the principal quantum number $n = n_r + l + 1$ in the nonrelativistic limit $\alpha = 0$ where $\gamma = l + 1$. The radial wave functions read

$$u_{n_r l}(r) = \sqrt{\frac{\Gamma(n_r + 2\gamma)}{2\nu n_r!}} \frac{(2\epsilon_{n_r l})^{\gamma+1/2}}{\Gamma(2\gamma)} r^{\gamma} \times {}_1F_1(-n_r, 2\gamma, 2\epsilon_{n_r l}\, r) e^{-\epsilon_{n_r l} r}, \tag{A3}$$

where

$$\epsilon_{n_r l} = \sqrt{1 - E_{n_r l}^2} = \frac{Z\alpha}{\mathcal{N}}. \tag{A4}$$

The total relativistic energy is given by

$$E_{n_r l} = \frac{\nu}{\mathcal{N}}. \tag{A5}$$

The binding energy reads

$$E_{n_r l} - 1 = -\frac{Z^2\alpha^2}{\mathcal{N}(\mathcal{N} + \nu)}. \tag{A6}$$

This writing minimizes rounding errors in numerical evaluations, as also observed in the Dirac case [13].

Mean values of powers of the radial coordinate are given by

$$\langle r \rangle = \frac{3\nu^2 - \gamma(\gamma - 1)}{2\nu\epsilon_{n_r l}}, \tag{A7}$$

$$\langle r^2 \rangle = \frac{5\nu^2 - 3\gamma(\gamma - 1) + 1}{2\epsilon_{n_r l}^2}, \tag{A8}$$

$$\left\langle \frac{1}{r} \right\rangle = \frac{\epsilon_{n_r l}}{\nu} = \frac{Z\alpha}{\nu\mathcal{N}}, \tag{A9}$$

$$\left\langle \frac{1}{r^2} \right\rangle = \frac{2\epsilon_{n_r l}^2}{\nu(2\gamma - 1)}. \tag{A10}$$

Expressions in atomic units are obtained for $E_{n_r l} - 1$ after multiplying by c^2 and for $\langle r^k \rangle$ after multiplying by $c^{-k} = \alpha^k$.

[1] D. Baye and P.-H. Heenen, J. Phys. A **19**, 2041 (1986).
[2] M. Vincke, L. Malegat, and D. Baye, J. Phys. B **26**, 811 (1993).
[3] D. Baye, Phys. Rep. **565**, 1 (2015).
[4] S. Quaglioni and P. Navrátil, Phys. Rev. Lett. **101**, 092501 (2008).
[5] T. Druet, D. Baye, P. Descouvemont, and J.-M. Sparenberg, Nucl. Phys. A **845**, 88 (2010).
[6] C. Romero-Redondo, S. Quaglioni, P. Navrátil, and G. Hupin, Phys. Rev. Lett. **117**, 222501 (2016).
[7] R. Lazauskas, Phys. Rev. C **97**, 044002 (2018).
[8] Shubhchintak and P. Descouvemont, Phys. Rev. C **105**, 024605 (2022).
[9] M. Hesse and D. Baye, J. Phys. B **32**, 5605 (1999).
[10] M. Hesse and D. Baye, J. Phys. B **36**, 139 (2003).
[11] D. Baye, J. Dohet-Eraly, and P. Schoofs, Phys. Rev. A **99**, 022508 (2019).
[12] D. Baye and J. Dohet-Eraly, Phys. Rev. A **103**, 022823 (2021).
[13] D. Baye, L. Filippin, and M. Godefroid, Phys. Rev. E **89**, 043305 (2014).
[14] L. Filippin, M. Godefroid, and D. Baye, Phys. Rev. A **90**, 052520 (2014).
[15] L. Filippin, M. Godefroid, and D. Baye, Phys. Rev. A **93**, 012517 (2016).
[16] D. Baye, Phys. Rev. A **92**, 042112 (2015).
[17] D. Baye, M. Hesse, and M. Vincke, Phys. Rev. E **65**, 026701 (2002).
[18] A. Messiah, *Quantum Mechanics* (Elsevier, North-Holland, Amsterdam 1962), Vol. 2.
[19] G. D. Mahan, *Quantum Mechanics in a Nutshell* (Princeton University Press, Princeton, 2009).
[20] D. Baye, J. Phys. B **28**, 4399 (1995).
[21] M. Abramowitz and I. A. Stegun, *Handbook of Mathematical Functions* (Dover, New York, 1965).
[22] G. Szegö, *Orthogonal Polynomials* (American Mathematical Society, Providence, RI, 1967).
[23] J. C. Light, I. P. Hamilton, and J. V. Lill, J. Chem. Phys. **82**, 1400 (1985).
[24] B. D. Shizgal and H. Chen, J. Chem. Phys. **104**, 4137 (1996).
[25] E. Tiesinga, P. J. Mohr, D. B. Newell, and B. N. Taylor, Rev. Mod. Phys. **93**, 025010 (2021).